Optimisation of wastewater treatments through combined geomaterials and natural soil filter: modelling tools

Marie Pettenati, N. Croiset, Géraldine Picot-Colbeaux, J. Casanova, Mohamed Azaroual, K. Besnard, N. Rampnoux

HAL Id: hal-03652347

https://hal-brgm.archives-ouvertes.fr/hal-03652347

Submitted on 26 Apr 2022

Optimisation of wastewater treatments through combined geomaterials and natural soil filter: modelling tools

M. Pettenati, N. Croiset, G. Picot-Colbeaux, J. Casanova, M. Azaroual, K. Besnard and N. Rampnoux

ABSTRACT

The main objective of this study is the establishment of innovative purification systems through the conceptualisation of reactive barriers in soil for artificial recharge of groundwater with treated wastewater. Numerical integration of hydrodynamics and biogeochemical processes controlling the effectiveness of this engineering system is applied to design soil column experiments. This leads to the elaboration of a combined aerobic/anaerobic environment to ensure the successive nitrification of rich ammonium wastewater and the denitrification mechanisms reducing NO_3^- according to heterotrophic denitrification and pyrite oxidation. A MIN3P reactive flow and transport model is used to reproduce an experimental flow-through column. Calculated concentrations of CH_2O and NO_3^- are consistent with experimental results. Agreement between model and experimental results makes it possible to understand major processes taking place in the column and optimises future treatment experiments.

Key words | denitrification, natural soil filter treatment, reactive transport modelling, wastewater reclamation

M. Pettenati (corresponding author)
N. Croiset
G. Picot-Colbeaux
J. Casanova
M. Azaroual
BRGM,
3 avenue C. Guillemin,
BP 36009,
45 060 Orléans,
France
E-mail: *m.pettenati@brgm.fr*

K. Besnard
N. Rampnoux
Veolia Environnement Recherche & Innovation
  SNC,
10 Rue Jacques Daguerre,
92500 Rueil-Malmaison,
France

INTRODUCTION

Throughout the world, health risks due to contaminated water from anthropic activities increase year by year. This uncontrolled overexploitation of water resources through industrial, agricultural and mining activities of the 21st century necessitates investigation of new wastewater treatments. Due to the scarcity and the accessibility of drinking water, especially in arid and semi-arid environments, reuse water remediation through optimised soil filter (soil reactive barrier) technology is being developed to forecast the feasibility of the MAR (Managed Aquifer Recharge) system in a regional context.

In this context, we are developing and operating successive pilot tests consisting of percolating wastewater in multilayer soil columns (natural soil with sand to ensure sufficiently high permeability) in order to improve effluent water quality. Impacts of the pilot scheme on the physicochemical and biogeochemical properties of porous medium are studied, such as reduced permeability or mobilisation of pollutants due to the change of redox conditions, which could lead to alteration of the treatment capacity (Greskowiak *et al.* 2005; Mayer *et al.* 2006; Miller *et al.* 2008).

In this paper, we concentrate our efforts on ammonium attenuation taking into account the nitrification and denitrification processes related to dissolved organic matter (DOM) degradation mechanisms in optimised natural soil column filters. First, wastewater ammonium oxidation in the case of water reclamation is an important process. However, in the overall cycle of N, nitrate (NO_3^-) is also of great importance because it is commonly found in groundwater due to agricultural activities and industrial processes (Jørgensen *et al.* 2009). Different techniques are used for NO_3^- removal in the case of wastewater reuse, such as ion exchange,

reverse osmosis and biological denitrification (André et al. 2011). Other than denitrification, biogeochemical processes are also the key factors controlling inorganic and organic pollutant mobility, such as pathogens, trace metals, metalloids, in natural soil environments. During these processes, microorganisms synthesise biomass. The microbial activity ensures the decomposition of bioavailable organic matter by oxidative breakdown of external organic substrates which provides the microorganisms with energy, nutrients and electrons (Hunter et al. 1998).

In this paper, we propose to use the results of pilot tests in order to implement reactive-transport code, new key (hydrological, chemical and biological) parameters. After 2 months of flow-through column experiments, the chemical data collected at the outlet of the column are used to calibrate a conceptual biogeochemical reactive-transport model. On the postulate that succession of unsaturated/saturated conditions is effective in the laboratory column, the hydrodynamic part of the MIN3P (Mayer et al. 2002; Gérard et al. 2008; Molins et al. 2008) is used to calibrate physical parameters controlling these two distinct hydrodynamic conditions on the top and bottom of the column. Then, geochemical analysis of the operating pilot allows us to determine DOM removal throughout the 2-month experiment. These values are used to consider organic matter degradation via a kinetically controlled redox process. Moreover, the geochemical part of the MIN3P code (Mayer et al. 2002; Gérard et al. 2008; Molins et al. 2008) is also used to estimate nitrification rates of ammonium in the wastewater considering the aerobic environment. Finally, reductive conditions are tested in order to ensure denitrification of the effluent. In this model the thermokinetic approach is integrated to take into account the redox disequilibrium of such organic systems. This first set of laboratory column experiments has been used to enrich the back and forth between field lab experiments and modelling.

EXPERIMENT DESCRIPTION

Depending on the composition of recharge wastewater enriched in ammonium (Figure 1, Table A) and DOM (no specific inoculum in injected water), a decision is made to
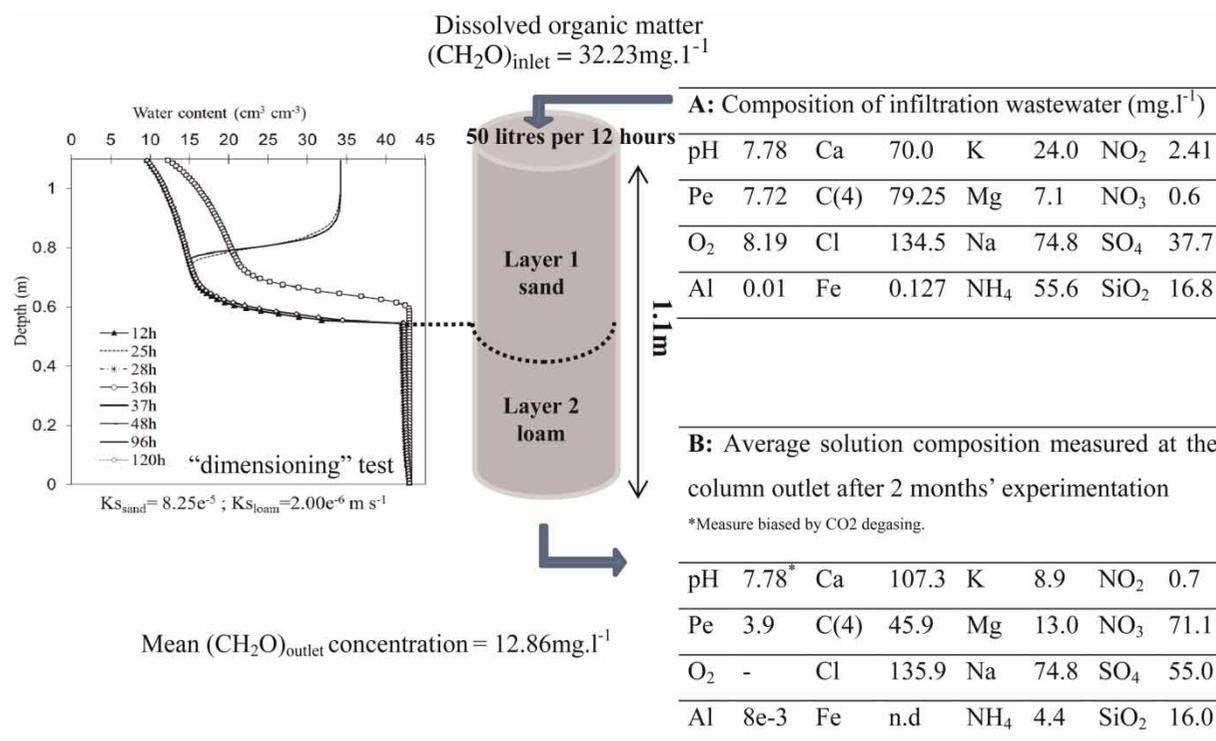

Dissolved organic matter $(CH_2O)_{inlet} = 32.23 mg.l^{-1}$

50 litres per 12 hours

$Ks_{sand} = 8.25e^{-5}$; $Ks_{loam} = 2.00e^{-6}$ m s^{-1}

Mean $(CH_2O)_{outlet}$ concentration = 12.86 mg.l^{-1}

A: Composition of infiltration wastewater (mg.l⁻¹)

pH	7.78	Ca	70.0	K	24.0	NO₂	2.41
Pe	7.72	C(4)	79.25	Mg	7.1	NO₃	0.6
O₂	8.19	Cl	134.5	Na	74.8	SO₄	37.7
Al	0.01	Fe	0.127	NH₄	55.6	SiO₂	16.8

B: Average solution composition measured at the column outlet after 2 months' experimentation

*Measure biased by CO2 degasing.

pH	7.78*	Ca	107.3	K	8.9	NO₂	0.7
Pe	3.9	C(4)	45.9	Mg	13.0	NO₃	71.1
O₂	-	Cl	135.9	Na	74.8	SO₄	55.0
Al	8e-3	Fe	n.d	NH₄	4.4	SiO₂	16.0

Figure 1 | Hydrodynamic parameter calibration and geochemical composition of laboratory column solutions.

create a 'bi-layer' column in the laboratory. The top layer is permeable enough to permit a relatively quick flow and a well-oxygenated environment. The layer underneath is less permeable and allows the establishment of anoxic conditions under permanent saturated conditions. Therefore, at a first attempt, we suggest that the first layer is sufficiently oxygenated to reach oxidising conditions.

In the lower part of the column, anaerobic conditions are established allowing the reduction of nitrate to nitrite and, ultimately, N_2 gas. Figure 1 shows the column experiment and the composition of the injected wastewater and the average composition of the outlet solution after 2 months (Figure 1, Table B).

After dimensioning tests performed with the hydrodynamic code MARTHE (Thiéry 1990), two successive infiltrations of 50 L of wastewater are added every 12 h in the 1.1 per 1 m cylindrical experimental column. Four sampling tests have been realised during 2 months for the outlet solution composition. An average composition is presented in Figure 1, Table B.

REACTIVE TRANSPORT CONCEPTUAL MODEL

Numerical integration of key factors controlling the establishment of sensitive microbial communities is used to design soil column experiments. Recommendations for developing a powerful column filter for water reclamation in the laboratory led to the modelling of multiple columns by using a 1D-reactive transport column utilising MIN3P (Mayer *et al.* 2002; Gérard *et al.* 2008).

The following text describes the conceptual model.

Variably saturated flow equation

The MIN3P is a reactive transport code which includes a range of kinetic and equilibrium geochemical and biogeochemical reactions (Mayer *et al.* 2002) with a formulation for multicomponent gas diffusion and advection (see Molins & Mayer 2007).

The nonlinear relationships between water content θ(m^3 m^{-3}), relative permeability k_r and pressure head $h = H - z$ (with H, the hydraulic head and z being the elevation with respect to datum) is expressed by the standard soil hydraulic functions given by van Genuchten (1980) (Equations (1) and (2)):

$$\theta = \theta_r + \frac{(\theta_s - \theta_r)}{(1 + (\alpha h)^n)^m} \tag{1}$$

$$k_r = \Theta + \left[1 - \left(1 - \Theta^{1/m}\right)^m\right]^2 \tag{2}$$

where θ_r (m^3 m^{-3}) defines the residual saturation of the aqueous phase, α(m^{-1}) is inversely related to the bubbling pressure, n and m are soil hydraulic function parameters, with $m = 1 - 1/n$. Θ is the effective saturation of the aqueous phase defined by Equation (3):

$$\Theta = \frac{\theta - \theta_r}{\theta_s - \theta_r} \tag{3}$$

Figure 2 summarises transport boundary conditions. In order to simplify the hydrodynamic part of the calculation and given the uncertainty of hydrodynamic parameters of laboratory experiments, the hydrodynamic soil properties are considered homogeneous and the physical unsaturated/saturated 'bilayer-column' is created by a fixed hydraulic head boundary condition at the bottom of the column.

Dissolution/precipitation reactions

Kinetics of dissolution/precipitation reactions for minerals are based on surface controlled rate expression (Table 1). The reaction rate is expressed by Equation (4):

$$R_i^m = -k_i^{m,\text{eff}} \left[1 - \left(\frac{\text{IAP}_i^m}{K_i^m}\right)^m\right]^n \tag{4}$$

where $k_i^{m,\text{eff}}$ is the rate constant k_i (mol m^{-2} s^{-1}) multiplied by the surface area (m^2 L^{-1}), IAP_i^m is the ion activity product and K_i^m is the thermodynamic equilibrium constant for the reaction (Lasaga 1998).

For this work, a simplified mineralogy similar to the actual composition of a natural soil and sand mixture (quartz, calcite, ferrihydrite and pyrite) is adopted for the conceptual model. We consider in the model only minerals that have a significant impact on the water geochemistry.
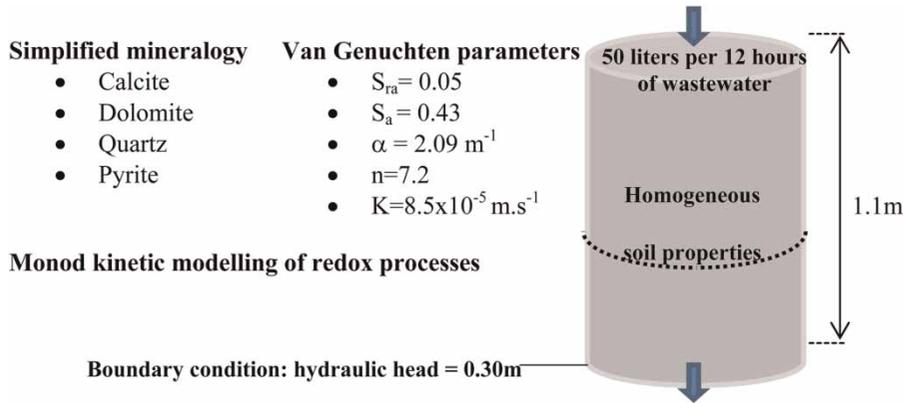
Simplified mineralogy
- Calcite
- Dolomite
- Quartz
- Pyrite

Van Genuchten parameters
- $S_{ra} = 0.05$
- $S_a = 0.43$
- $\alpha = 2.09$ m^{-1}
- $n = 7.2$
- $K = 8.5 \times 10^{-5}$ m.s^{-1}

Monod kinetic modelling of redox processes

Boundary condition: hydraulic head = 0.30m

50 liters per 12 hours of wastewater

Homogeneous soil properties

1.1m

Figure 2 | Conceptual MIN3P reactive-transport model.

Table 1 | Dissolution/precipitation kinetic reactions parameters

Minerals	Log rate coefficient [log (mol.L^{-1} s^{-1})][a]	Surface area (m^2 L^{-1})
Quartz		
$SiO_2 + 2H_2O \rightarrow H_4SiO_4$	$\log k_{Quartz} = -13.40$	133
Calcite		
$CaCO_3 + H^+ \rightarrow Ca^{2+} + HCO_3^-$	$\log k_{Calcite} = -5.81$	0.75
Ferrihydrite		
$Fe^{3+} + 3H_2O \rightarrow Fe(OH)_3 + 3H^+$	$\log k_{Ferrihydrite} = -10.19$	3.5×10^3
Pyrite		
$FeS_2 + \frac{7}{2}O_2(aq) + H_2O \rightarrow 2SO_4^{2-} + 2H^+ + Fe^{2+}$	$S_i = 1.66 \times 10^{-7}; r_i^p = 7.0 \times 10^{-6}$ m$\\D_{il}^m = 2.41 \times 10^{-9}$ m² s^{-1}$\\r_i^r = 6.93 \times 10^{-6}$ m; $v_{il}^m = 3.5$	

[a]From Palandri & Kharaka (2004).

The kinetic parameters selected for these minerals are given in Table 1. MIN3P allows the use of the shrinking core model (Nicholson *et al.* 1990) to describe mineral dissolution reactions. Due to the accumulation of alteration products on the mineral surface, the oxidation of pyrite by dissolved oxygen may be described using this model. A rate expression based on the shrinking core model can be expressed as Equation (5):

$$R_i^m = -10^3 S_i \frac{r_i^p}{(r_i^p - r_i^r)r_i^r} \frac{D_{il}^m}{v_{il}^m}[O_2(aq)] \qquad (5)$$

In this rate expression 10^3 is a conversion factor [L m^{-3}], S_i is scaling factor including the tortuosity of the surface coating or altered rim on the mineral surface, r_i^p is the radius of the particle, r_i^r is the radius of the unreacted portion of the particle, D_{il}^m is the free phase diffusion coefficient of the primary reactant in water (in this case $O_2(aq)$ and v_{il}^m is the stoichiometric coefficient of oxygen in the reaction equation (Table 1). In the literature, many authors report that a pyrite-bearing rock can contribute with significant high-rate reaction to nitrate reduction (Pauwels *et al.* 1998; Torrento *et al.* 2008; Pauwels *et al.* 2010; André *et al.* 2011), mediated by the autotrophic bacteria. However, pyrite oxidation is most likely dominated by the reaction with oxygen in a well-aerated porous media.

Kinetic modelling of redox processes

Heterotrophic denitrification involving organic matter (Table 2) is a process reported on by Pauwels *et al.* (2001)

Table 2 | Monod kinetic reaction parameters

	Monod parameters (mol L^{-1})[a]			Rate coefficient (mol L^{-1} s^{-1})[b]
	(K_{CH2O})	(K_j)	(K_{inhib})	
$NH_4^+ + 2O_2 \rightarrow NO_3^- + H_2O + 2H^+$	–	$K_{NH_4^+} = 1.7 \times 10^{-5}$ $K_{O_2} = 1.9 \times 10^{-4}$	–	1×10^{-8}
$CH_2O + O_2 \rightarrow CO_3^{2-} + 2H^+$	1.6×10^{-4}	$K_{O_2} = 5.0 \times 10^{-5}$	–	2.5×10^{-9}
$CH_2O + 4/5NO_3^- \rightarrow 2/5N_2 + CO_3^{2-} + 6/5H^+ + 2/5H_2O$	1×10^{-5}	$K_{NO_3^-} = 2.3 \times 10^{-5}$	$K_{inhib} = 1.6 \times 10^{-5}$	1.5×10^{-8}

[a]Values are from range reported in the literature (see Miller et al. 2008).
[b]Used to fit experimental results.

and Pauwels & Talbo (2004). This approach needs to consider kinetics of intra-aqueous redox reactions.

Kinetic modelling of redox processes included in the MIN3P code is used in order to kinetically control the redox transformation for the principal electron acceptor (EA).

In this study, DOM (CH_2O) is considered to be the ultimate source of chemical energy for microbial and inorganic redox reaction. The biodegradation of organic substrates is represented by a series of reactions (Table 2) and degradation kinetic is assumed to be Monod (1949) type: for example, the equation to determine the rate of aerobic respiration is described by Equation (6):

$$R_{max}(CH_2O) = k \frac{[CH_2O]}{[CH_2O] + K_{CH_2O}} \times \frac{[EA]_{O_2}}{[EA]_{O_2} + K_{O_2}} \quad (6)$$

where $R_{max}(CH_2O)$ is the maximum rate of organic matter degradation for EA_j, k is the maximum specific rate of substrate utilisation (mol L^{-1} s^{-1}), K_{CH2O} is the half-saturation constant for the substrate DOM (mol L^{-1}), K_j is the half-saturation constant for the electron acceptor EA_j (mol L^{-1}) and $[EA]_j$ indicates concentration (mol L^{-1}). For specific denitrification reaction, an additional inhibition term is added to the Monod equation, such as:

$$R_{max}(NO_3^-) = k \frac{[CH_2O]}{[CH_2O] + K_{CH_2O}} \times \frac{[EA]_{NO_3^-}}{[EA]_{NO_3^-} + K_{NO_3^-}}$$
$$\times \frac{K_{inhib.}}{[H^+] + K_{inhib.}} \quad (7)$$

RESULTS AND DISCUSSION

Figure 3(a) shows the saturated state of the lower part of the column and the unsaturated state of the top of the column. The saturation state of the upper part of the column varies between two 12-hourly injections and reaches hydrodynamic steady state after two injections.
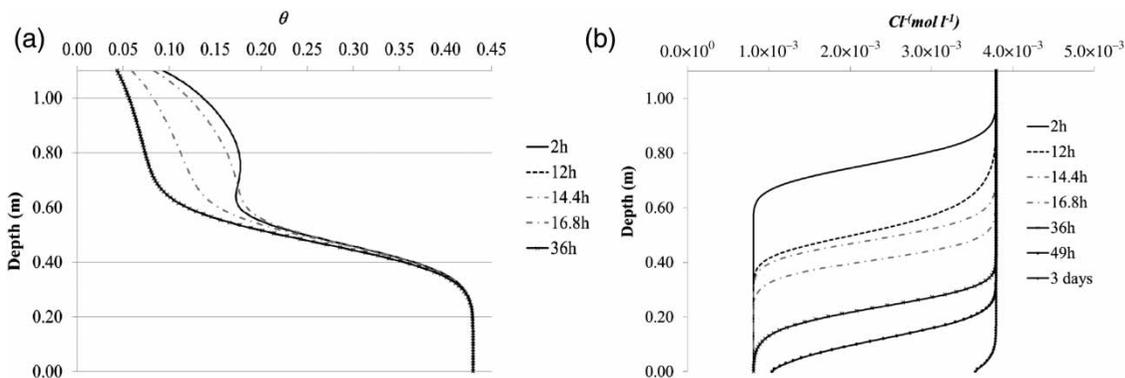

Figure 3 | (a) Water content S_{ea} versus depth after 36 h (permanent hydrological state); (b) non-reactive Cl$^-$ versus depth after 3 days.

The global residence time of the solution in the column is up to 3 days as shown by the Cl^- concentration versus depth (Figure 3(b)).

Figure 4 confirms that O_2 is consumed during the infiltration, especially in the saturated part of the column.

More than 30 numerical tests have been performed in order to determine kinetic rates of redox processes
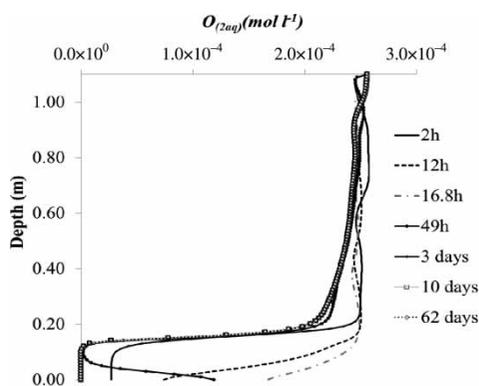

Figure 4 | O_2 concentration versus depth after 62 days.

(Table 2). The implementation of CH_2O degradation by aerobic respiration and heterotrophic denitrification allows reproduction of the CH_2O decrease at the outlet of the column (Figure 5(a)). Concentration oscillations observed in the solution at the outlet of the column after 3 days of percolation are due to the 12-hourly wastewater injections. The model is in good accordance with nitrification processes and reproduces NO_3^- concentration at the outlet of the column (Figure 5(b)): only part of injected NH_4^+ is transformed into NO_3^-. NH_4^+ sorption on exchangeable fraction of clays is not included in the model. This process is of great importance for NH_4^+ immobilisation in soils (Vogeler et al. 2011); this is why NH_4^+ model concentration is too high compared to the concentration measured at the outlet of the laboratory column (Figure 5(c)). The strong decrease of O_2 followed immediately by the production of N_2 illustrates the part of denitrification due to the degradation of CH_2O. To be consistent with CH_2O measurements (see Table 1), rate constants for aerobic respiration and heterotrophic denitrification had to be minimised.
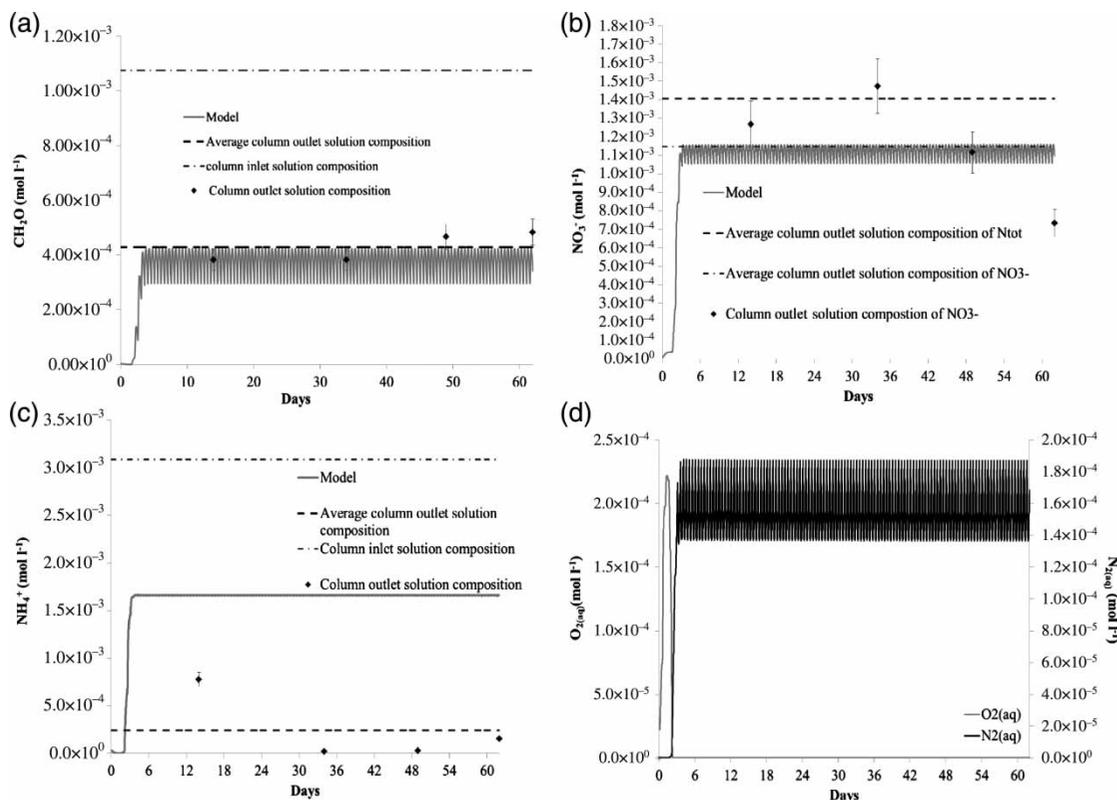

Figure 5 | CH_2O, NH_4^+, NO_3^-, $O_{2(aq)}$ and $N_{2(aq)}$, concentration in the last cell of the column ($z = 0$). Wastewater and average laboratory column compositions are also reported.

As SO_4^{2-} concentration is greater at the column outlet (Table 1), pyrite oxidation is assumed to take place in the column.

Calculated concentration of SO_4^{2-} is only close to the final measured concentration at the outlet of the column (Figure 6(a)). The kinetic of pyrite oxidation strongly depends on O_2 gas diffusion in the unsaturated/saturated conditions (Xu et al. 2000). The difficulty is to reproduce realistic O_2 diffusion in the heterogeneous and complex porous media with a conceptual simplified model. The difference between measured and simulated SO_4^{2-} concentrations can be imputed to this mechanism. Fe^{2+} produced by pyrite oxidation precipitates as ferrihydrite (Figure 6(b)) resulting in iron concentration values under the detection limit at the outlet of the column (Figure 1, Table B).

The differences between measured values for pH and HCO_3^- and calculated ones (Figure 6(c), (d)) are due to the high pCO_2 calculated in the model and produced by
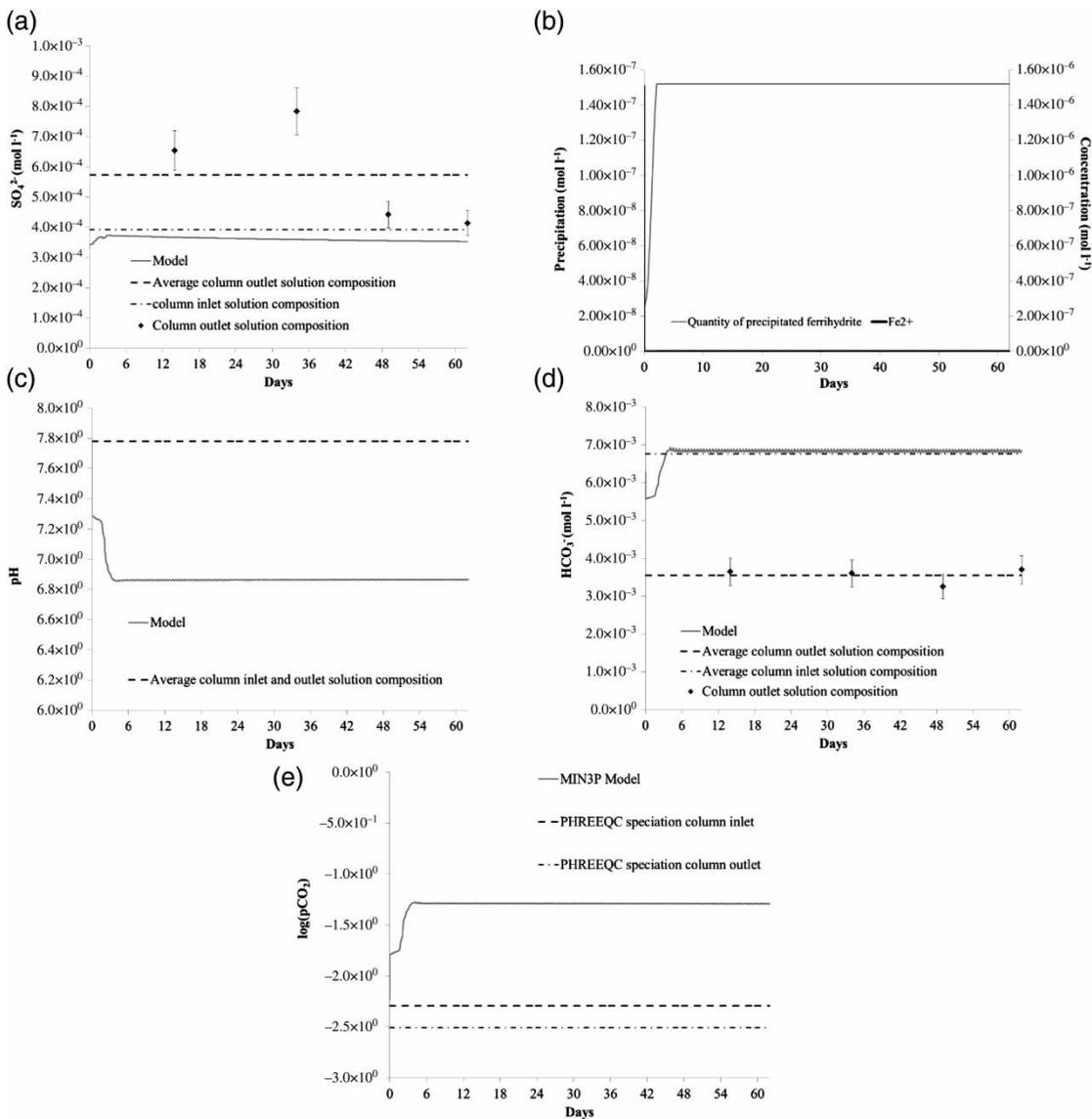

Figure 6 | SO_4^{2-}, Fe^{2+}, precipitation of ferrihydrite, $\log pCO_2$ (calculated with PHREEQC, Parkhurst & Appelo (1999)), HCO_3^- and pH in the last cell of the column ($z = 0$). Wastewater and average laboratory column compositions are also reported.

bacteria activity (Figure 6(e)). In the laboratory, solutions at the outlet of the column are sampled without considering pressure (disconnection between the column and the sampling bottle). The difference in pCO_2 between model and sampling can be explained by a degasing phenomenon before the sampling. The pCO_2 is expected to be higher and pH value more acidic in the environment of soil pore solution at the bottom of the experimental column.

CONCLUSION AND OUTLOOK

Through successive pilot experiments, we have attempted to distinguish the effective natural capacity of soil to buffer organic and inorganic pollutants (pathogens, heavy metals, nitrogen compounds, etc.) in order to optimise the main processes controlling the drop of pollutants with eventually the addition of geomaterials in the system. The reactive-transport modelling allows us to identify these processes to predict the future geochemical behaviour of the optimised soil filter. First geochemical model results demonstrate the possibility of aerobic respiration, nitrification, heterotrophic denitrification and pyrite oxidation. The model shows the possible precipitation of ferrihydrite. Future simulations have to be performed, including iron hydroxide surface complexation mechanisms, in order to test trace element mobility. The hydrodynamic model allows us to determine the physical parameters controlling the saturation state of experimental columns. Future laboratory experiments will be dedicated to the monitoring and adjustment of hydrodynamic parameters to ensure the succession of non-saturated/saturated conditions in the natural soil filter column.

ACKNOWLEDGEMENTS

REFERENCES

André, L., Pauwels, H., Dictor, M.-C., Parmentier, M. & Azaroual, M. 2011 Experiments and numerical modelling of microbially-catalysed denitrification reactions. Chem. Geol. **287**, 171–181.

Hunter, K. S., Wang, Y. F. & Van Cappellen, P. 1998 Kinetic modeling of microbially-driven redox chemistry of subsurface environments: coupling transport, microbial metabolism and geochemistry. J. Hydrol. **209**, 53–80.

Gérard, F., Mayer, K. U., Hodson, M. J. & Ranger, K. 2008 Modelling the biogeochemical cycle of silicon in soil: application to a temperate forest ecosystem. Geochim. Cosmochim. Acta **72**, 741–758.

Greskowiak, J., Prommer, H., Massmann, G., Johnston, C. D., Nutzmann, G. & Pekdeger, A. 2005 The impact of variably saturated conditions on hydrogeochemical changes during artificial recharge of ground water. Appl. Geochem. **20**, 1409–1426.

Jørgensen, C. J., Jacobsen, O. S., Elberling, B. & Aamand, J. 2009 Microbial oxidation of pyrite coupled to nitrate reduction in anoxic groundwater sediment. Environ. Sci. Technol. **43**, 4851–4857.

Lasaga, A. C. 1998 Kinetic Theory in the Earth Sciences. Princeton University Press, Princeton.

Mayer, K. U., Frind, E. O. & Blowes, D. W. 2002 Multicomponent reactive transport modelling in variably saturated porous media using a generalized formulation for kinetically controlled reactions. Water Resour. Res. **38**, 1174–1195.

Mayer, K. U., Benner, S. G. & Blowes, D. W. 2006 Process based reactive transport modeling of a permeable reactive barrier for the treatment of mine drainage. J. Contam. Hydrol. **85**, 195–211.

Miller, G. R., Rubin, Y., Mayer, K. H. & Benito, P. H. 2008 Modeling vadose zone processes during land application of food-processing waste water in California's Central Valley. J. Environ. Qual. **37**, S43–S47.

Molins, S. & Mayer, K. U. 2007 Coupling between geochemical reactions and multicomponent gaz and solute transport in unsaturated media: a reactive transport modeling study. Water Resour. Res. **43**, W05435.

Molins, S., Mayer, K. U., Scheutz, C. & Kjeldsen, P. 2008 Transport and reaction processes affecting the attenuation of landfill gas in cover soils. J. Environ. Qual. **37**, 458–468.

Monod, J. 1949 The growth of bacterial cultures. Annu. Rev. Microbiol. **3**, 371–393.

Nicholson, R. V., Gillham, R. W. & Reardon, E. J. 1990 Pyrite oxidation in carbonate-buffered solution: 2. Rate control by oxide coatings. Geochim. Cosmochim. Acta **54**, 395–402.

Palandri, J. L. & Kharaka, Y. K. 2004 A compilation of rate parameters of water-mineral interaction kinetics for application to geochemical modeling: US Geological Survey Water-Resources Investigations Report 04-1068. Available

from: http://pubs.usgs.gov/of/2004/1068/pdf/
OFR_2004_1068.pdf.

Parkhurst, D. L. & Appelo, C. A. J. 1999 User's Guide to
PHREEQC (Version 2) – A Computer Program for
Speciation, Batch-Reaction, One-Dimensional Transport,
and Inverse Geochemical Calculations, Water Resources
investigations report, 99-4259. Available from: http://
wwwbrr.cr.usgs.gov/projects/GWC_coupled/phreeqc/index.
html.

Pauwels, H. & Talbo, H. 2004 Nitrates concentration in
wetlands: assessing the contribution of different water
bodies from anion concentrations. *Water Res.* **38**,
1019–1025.

Pauwels, H., Kloppmann, W., Foucher, J.-C., Martelat, A. &
Fritsche, V. 1998 Field tracer test for denitrification in
a pyrite-bearing schist aquifer. *Appl. Geochem.* **13** (6),
767–778.

Pauwels, H., Lachassagne, P., Bordenave, P., Foucher, J.-C. &
Martelat, A. 2001 Temporal variability of nitrate
concentration in a schist aquifer and transfer to surface
waters. *Appl. Geochem.* **16** (6), 583–596.

Pauwels, H., Ayraud, V., Aquilina, L. & Molénat, J. 2010 The fate
of nitrogen and sulfur in hard-rock aquifers as shown by
sulfate-isotope tracing. *Appl. Geochem.* **25** (1), 105–115.

Thiéry, D. 1990 Software MARTHE, Modelling of aquifers with a
rectangular grid in transient state for hydrodynamic
calculations of heads and flows, Release 4.3, Report BRGM/
R32548. Available from: http://www.brgm.fr/pdf/logiciels/
Marthe.pdf.

Torrento, C., Southam, G., Urmeneta, J., Cama, J. & Spmer, A.
2008 Anaerobic nitrate-dependent oxidation of pyrite
mediated by *Thiobacillus denitrificans*. *Goldschmidt Confer.
GCA* **71**, A1032.

van Genuchten, M. T. 1980 A closed-form equation for predicting
the hydraulic conductivity of unsaturated soils. *Soil Sci. Soc.
Am. J.* **44**, 892–898.

Vogeler, I., Cichota, R., Snow, V. O., Dutton, T. & Daly, B. 2011
Pedotransfer functions for estimating ammonium adsorption
in soils. *Soil Sci. Soc. Am. J.* **75**, 324–331.

Xu, T., White, S. P., Pruess, K. & Brimhall, G. H. 2000 Modeling
pyrite oxidation in saturated and unsaturated subsurface flow
systems. *Transp. Porous Med.* **39**, 25–56.